

Lorentz noninvariant neutrino oscillations without neutrino mass

K. Whisnant

Department of Physics and Astronomy, Iowa State University, Ames, IA 50011, USA

The bicycle model of Lorentz noninvariant neutrino oscillations without neutrino masses naturally predicts maximal mixing and a $1/E$ dependence of the oscillation argument for $\nu_\mu \rightarrow \nu_\tau$ oscillations of atmospheric and long-baseline neutrinos, but cannot also simultaneously fit the data for solar neutrinos and KamLAND. We examine all nineteen possible structures of the Standard Model Extension for Lorentz noninvariant oscillations of massless neutrinos that naturally have a $1/E$ dependence at high neutrino energy. Due to the lack of any evidence for direction dependence, we consider only direction-independent oscillations. Although we find a number of models with a $1/E$ dependence for atmospheric and long-baseline neutrinos, none can also simultaneously fit solar and KamLAND data.

1. Introduction

Neutrino data from atmospheric, long-baseline, solar and reactor experiments are easily explained by oscillations of three active, massive neutrinos [1]. Lorentz-invariance and CPT violating interactions originating at the Planck scale can also lead to neutrino oscillations. The Standard Model Extension (SME) [2] includes all such interactions that may arise from spontaneous symmetry breaking but still preserve Standard Model gauge invariance and power-counting renormalizability. Studies of neutrino oscillations with Lorentz invariance violation have been made both for massive [3–5] and massless [6–8] neutrinos. A model with nonrenormalizable Lorentz invariance violating interactions and neutrino mass has also been proposed [9]. However, no viable model has been found that does not require at least one nonzero neutrino mass. The purpose of this paper is to determine if Lorentz invariance violation alone can account for the verified oscillation phenomena seen in atmospheric, long-baseline, solar and reactor neutrinos. We do not attempt to fit the possible oscillation signals seen in the LSND [10] and MiniBooNE [11] experiments. Our complete results are given in Ref. [12].

In the SME, the evolution of massless neutrinos in vacuum may be described by the effective Hamiltonian [6]

$$(h_{eff})_{ij} = E\delta_{ij} + \frac{1}{E} [a_L^\mu p_\mu - c_L^{\mu\nu} p_\mu p_\nu]_{ij}, \quad (1)$$

where $p_\mu = (E, -E\hat{p})$ is the neutrino four-momentum, \hat{p} is the neutrino direction, i, j are flavor indices, and $a_L \rightarrow -a_L$ for antineutrinos. The coefficients a_L have dimensions of energy and the c_L are dimensionless. Direction dependence of the neutrino evolution enters via the space components of a_L and c_L , μ or $\nu = X, Y, Z$, while direction independent terms have $\mu = \nu = T$. The Kronecker delta term on the right-hand side of Eq. (1) may be ignored since oscillations are insensitive to terms in h_{eff} proportional to the identity.

The two-parameter bicycle model [6] can be defined as follows: $(c_L)_{ij}$ has only one nonzero element in flavor space and the only nonzero $(a_L)_{ij}$ are $(a_L)_{e\mu} = (a_L)_{e\tau}$. These interactions can be nonisotropic, which could lead to different oscillation parameters for neutrinos propagating in different directions. In Ref. [8] it was shown that the pure direction-dependent bicycle model is ruled out by solar neutrino data alone, while a combination of atmospheric, solar and long-baseline neutrino data excludes the pure direction-independent case. A mixture of direction-dependent and direction-independent terms (with 5 parameters) is also excluded when KamLAND data are added [8].

The key feature of the bicycle model is that even though the terms in h_{eff} are either constant or proportional to neutrino energy, at high neutrino energies there is a seesaw type mechanism that leads to $1/E$ behavior for the oscillation argument for atmospheric and long-baseline neutrinos. In this paper we examine the general case of direction-independent Lorentz invariance violation in the Standard Model Extension for three neutrinos without neutrino mass, *i.e.*, Eq. (1) with only c_L^{TT} and a_L^T terms. We do not consider possible direction-dependent terms since there is no evidence for direction dependence in neutrino oscillation experiments (see, *e.g.*, the experiments in Ref. [13] and the analysis of Ref. [6]). For notational simplicity we henceforth drop the L subscript and T superscripts from the c_L^{TT} and a_L^T in our formulae.

We first look for textures of the c_{ij} in flavor space that allow a $1/E$ dependence of the oscillation argument at high neutrino energy. We then check the phenomenology for atmospheric, long-baseline, solar and reactor neutrino experiments. We were unable to find any texture of h_{eff} that could simultaneously fit all the data.

In Sec. 2 we review the constraints on the direction-independent bicycle model. In Sec. 3 we list all possible textures of the c coefficients and find which ones allow a $1/E$ dependence of the oscillation argument at high neutrino energies. For those that do, we first check the oscillation amplitude for atmospheric and long-baseline

neutrinos, and if suitable parameters are found we then check the ability of the model to fit KamLAND and solar neutrino data. In Sec. 4 we summarize our results.

2. Neutrino oscillations in the bicycle model

Neutrino oscillations occur due to eigenenergy differences in h_{eff} and the fact that the neutrino flavor eigenstates are not eigenstates of h_{eff} . In our generalization of the direction-independent bicycle model,

$$h_{eff} = \begin{pmatrix} -2cE + 2a_{ee} & a_{e\mu} & a_{e\tau} \\ a_{e\mu} & 0 & 0 \\ a_{e\tau} & 0 & 0 \end{pmatrix}, \quad (2)$$

where the c term is CPT -even and the a_{ij} terms are CPT -odd. The simple two-parameter bicycle model [6] has $a_{e\tau} = a_{e\mu}$ and $a_{ee} = 0$. We allow $a_{e\mu}$ to be different from $a_{e\tau}$ so that mixing of atmospheric neutrinos may be (slightly) nonmaximal. The a_{ee} term allows an adjustment of the oscillation probabilities of low-energy solar neutrinos [6].

For large E , appropriate for atmospheric and long-baseline neutrinos, if $a^2 \equiv a_{e\mu}^2 + a_{e\tau}^2 \ll (cE)^2$, then the only appreciable oscillation is

$$P(\nu_\mu \leftrightarrow \nu_\tau) \simeq \sin^2 2\phi \sin^2(\Delta_{32}L/2), \quad (3)$$

where $\Delta_{32} \simeq a^2/(2cE)$ and $\tan \phi = a_{e\mu}/a_{e\tau}$. The energy dependence of the oscillation argument in this limit is the same as for conventional neutrino oscillations due to neutrino mass differences, with an effective mass-squared difference $\delta m_{eff}^2 = a^2/c$. The measured value for δm_{eff}^2 in atmospheric and long-baseline experiments then places a constraint that relates a and c .

If E is not too large, then the approximation in Eq. 3 does not apply. Furthermore, in matter there is an additional term due to coherent forward scattering [14], which adds a $\sqrt{2}G_F N_e$ term to the ν_e - ν_e element of h_{eff} , where N_e is the electron number density. For adiabatic propagation in the sun, the fact that the ^8B neutrinos have an oscillation minimum $P_{min} \simeq 0.30$ fixes a to be $b\sqrt{2P_{min}/(1-2P_{min})} = 2.1 \times 10^{-12}$ eV, where $b \equiv G_F N_e^0/(2\sqrt{2}) = 1.7 \times 10^{-12}$ eV.

At very low energies the solar neutrino oscillation probability is $P \approx 1 - \frac{1}{2} \sin^2 2\theta_{12} \approx 0.57$, where θ_{12} is the usual solar neutrino mixing angle [16]. This gives two possible values for a_{ee} , either $0.20b$ or $-2.2b$.

Finally, the ^8B probability reaches the minimum at $E_{min} = (a_{ee} + b)/c$, which must occur in the energy region of the ^8B solar neutrinos ($E_{min} \approx 10$ MeV), which fixes the magnitude of c to be $|c| = (a_{ee} + b)/E_{min} = 1.2 b/E_{min} \approx 2.0 \times 10^{-19}$.

We may now calculate the value of the atmospheric δm_{eff}^2 inferred from solar neutrino data: $\delta m^2 = a^2/c = 2.2 \times 10^{-5}$ eV², which is two orders of magnitude below the measured value. Therefore the direction-independent bicycle model is excluded.

3. Other textures for h_{eff}

3.1. Classification of models

There are six possible c coefficients in h_{eff} : three real diagonal coefficients and three complex off-diagonal coefficients (the remaining three off-diagonals are fixed by the hermiticity of h_{eff}). Therefore there are $2^6 = 64$ possible c textures for h_{eff} . Since the high-energy behavior of h_{eff} is determined by the c coefficients, we classify the models by the number of nonzero c there are in h_{eff} . Within each main class there are distinct subclasses which depend on the diagonal/off-diagonal structure; within each subclass there are textures that differ only by permutation of the flavor indices. In all there are 19 subclasses, which are listed in Table I.

We note that we may subtract any quantity proportional to the identity from h_{eff} , since common phases in the neutrino equations of motion do not affect the oscillations. In this way a diagonal element may be removed or moved from one position to another. Then it is not hard to see that the following subclasses are strictly equivalent: $3A \leftrightarrow 2A$, $3C \leftrightarrow 3B$, $4A \leftrightarrow 3B$, $4C \leftrightarrow 4B$, $5A \leftrightarrow 4B$ and $6 \leftrightarrow 5B$.

Table I: A list of the 64 possible c textures for h_{eff} . The number in the subclass name corresponds to the number of nonzero c , while the letters indicate a distinct diagonal/off-diagonal structure (up to flavor permutation), if applicable. A D_i in the structure column indicates that a diagonal c_{ii} is nonzero, while an O_{jk} indicates that off-diagonal c_{jk} is nonzero. Different latin indices in each case are distinct, *e.g.*, in the structure $D_i O_{jk}$ the diagonal element does not share a row or column with the off-diagonal element, whereas for $D_i O_{ij}$ it does.

Number of Subclass nonzero c		Structure	Number of flavor permutations
0	0	—	1
1	1A	D_i	3
	1B	O_{ij}	3
2	2A	$D_i D_j$	3
	2B	$D_i O_{ij}$	6
	2C	$D_i O_{jk}$	3
	2D	$O_{ij} O_{ik}$	3
3	3A	$D_i D_j D_k$	1
	3B	$D_i D_j O_{ij}$	3
	3C	$D_i D_j O_{ik}$	6
	3D	$D_i O_{ij} O_{ik}$	3
	3E	$D_j O_{ij} O_{ik}$	6
	3F	$O_{ij} O_{ik} O_{jk}$	1
4	4A	$D_i D_j D_k O_{ij}$	3
	4B	$D_i D_j O_{ij} O_{ik}$	6
	4C	$D_i D_j O_{ik} O_{jk}$	3
	4D	$D_i O_{ij} O_{ik} O_{jk}$	3
5	5A	$D_i D_j D_k O_{ij} O_{ik}$	3
	5B	$D_i D_j O_{ij} O_{ik} O_{jk}$	3
6	6	$D_i D_j D_k O_{ij} O_{ik} O_{jk}$	1

3.2. Method for analyzing textures

Our analysis proceeds as follows. We assume that $|c_{ij}E| \gg |a_{k\ell}|$ for any (i, j, k, ℓ) for the high energies of atmospheric and long-baseline neutrinos. This assumption is justified since if any a is similar in magnitude to the cE at high energies, then at lower energies (such as for reactor neutrinos) the a terms will dominate and the oscillation arguments will be energy-independent, contrary to the KamLAND data, which measured a spectral distortion (similarly, solar neutrinos would also not have an energy-dependent oscillation probability, as they must). Furthermore, for the sake of naturalness, we assume that the nonzero c coefficients are all the same order of magnitude, and that likewise the nonzero a coefficients are also the same order of magnitude.

Although for each texture the number of nonzero c is determined, initially we place no restrictions on the a . We note that if all off-diagonal c are nonzero, then by a redefinition of neutrino phases and adding a term proportional to the identity we may take all off-diagonal c to be real and positive, except for one off-diagonal c that is complex (which we take to be $c_{e\tau}$ unless otherwise noted). If any off-diagonal c is zero, the nonzero off-diagonal c may all be taken as real and positive.

A key feature of the bicycle model was that even though the terms in the effective Hamiltonian were either proportional to energy or constant in energy, one eigenvalue difference was proportional to E^{-1} , which mimics the energy dependence of the oscillations of atmospheric and long-baseline neutrinos. Having an eigenvalue difference proportional to E^{-1} means that if the eigenvalues are expanded in a power series in neutrino energy,

$$\lambda_i = \sum_{j=0}^{\infty} a_{ij} E^{1-j}, \quad \text{for } i = 1, 2, 3 \quad (4)$$

then two eigenvalues must be degenerate at leading order in E (linear in E), and at the next order in energy

(E^0 , independent of energy). Therefore in our analysis of more general three-neutrino models with Lorentz invariance violation, we look for model parameters that satisfy these conditions. Since an L/E dependence has been seen over many orders of magnitude in neutrino energy [17], it seems likely that this is the only way the Hamiltonian in Eq. (1) will be able to fit all atmospheric and long-baseline neutrino data.

For each texture we expand the eigenvalues of h_{eff} in powers of E (as in Eq. 4), where the leading E^1 behavior comes from the dominant cE terms. Since we want $1/E$ behavior for at least one oscillation argument, we require that two of the eigenvalues be degenerate to order E^0 , with the first nonzero difference occurring at order E^{-1} . In all cases this requirement puts constraints on the c and a coefficients. In our calculations we first find the eigenvalues to order E^1 and impose the constraint that two eigenvalues must be degenerate; then we find the eigenvalues of the simplified h_{eff} to order E^0 and again impose the degeneracy condition. In this way the expressions for the eigenvalues to order E^{-1} will be made as simple as possible at each stage of the calculation.

If the appropriate $1/E$ behavior can be achieved, the mixing angles are then calculated to determine if ν_μ 's have maximal mixing and ν_e small mixing for atmospheric and long-baseline neutrinos. If the model is still viable, the energy dependences of the oscillations of solar and KamLAND neutrinos are then checked for consistency.

At any time we are allowed to subtract a constant times the identity matrix from h_{eff} , so that some classes of models are equivalent to others.

3.3. Models with $1/E$ behavior at high energies

Only Classes 1A, 2C, 3B, 3F, 4D and 5B allow $1/E$ dependence of an eigenvalue difference at high neutrino energies. As an example of a class that does not have $1/E$ behavior, the effective Hamiltonian in Class 1B is

$$h_{eff} = \begin{pmatrix} a_{ee} & cE + a_{e\mu} & a_{e\tau} \\ cE + a_{e\mu}^* & a_{\mu\mu} & a_{\mu\tau} \\ a_{e\tau}^* & a_{\mu\tau}^* & a_{\tau\tau} \end{pmatrix}, \quad (5)$$

where $c_{e\mu} \equiv c$ may be taken as real and positive. The eigenvalues to order E^1 are then $\lambda_1, \lambda_2 = \pm|c|E$ and $\lambda_3 = 0$. Since these are all different at leading order in E , they cannot give an oscillation argument proportional to E^{-1} at high energies, and this case is not allowed.

For Class 1A the effective Hamiltonian is

$$h_{eff} = \begin{pmatrix} cE + a_{ee} & a_{e\mu} & a_{e\tau} \\ a_{e\mu}^* & a_{\mu\mu} & a_{\mu\tau} \\ a_{e\tau}^* & a_{\mu\tau}^* & a_{\tau\tau} \end{pmatrix}, \quad (6)$$

where $c_{ee} \equiv c$ may be taken as real and positive. The eigenvalues to order E^0 are then $\lambda_1 = cE + a_{ee}$ and $\lambda_2, \lambda_3 = \frac{1}{2}[a_{\mu\mu} + a_{\tau\tau} \pm \sqrt{(a_{\mu\mu} - a_{\tau\tau})^2 + 4|a_{\mu\tau}|^2}]$. The difference $\lambda_2 - \lambda_3$ can only be made zero to order E^0 if $a_{\mu\mu} = a_{\tau\tau}$ and $|a_{\mu\tau}| = 0$. Then $a_{\tau\tau}$ times the identity may be subtracted from h_{eff} ; if $a_{ee} - a_{\tau\tau}$ is redefined as a_{ee} , this case reduces to the generalized bicycle model described in Sec. 2, which is excluded by the combined data.

For Class 2C we have

$$h_{eff} = \begin{pmatrix} a_{ee} & a_{e\mu} & c_{e\tau}E + a_{e\tau} \\ a_{e\mu}^* & c_{\mu\mu}E & a_{\mu\tau} \\ c_{e\tau}E + a_{e\tau}^* & a_{\mu\tau}^* & a_{\tau\tau} \end{pmatrix}, \quad (7)$$

where $c_{\mu\mu}$ and $c_{e\tau}$ may be taken as real and positive, and we have subtracted a term proportional to the identity so that $a_{\mu\mu} = 0$. The eigenvalues at leading order are $\lambda_1, \lambda_2 = \mp c_{e\tau}E$ and $\lambda_3 = c_{\mu\mu}E$. Degeneracy requires $c_{e\tau} = c_{\mu\mu}$. The oscillation probabilities are approximately given by

$$P(\nu_\mu \rightarrow \nu_\mu) = 1 - \sin^2 2\theta \sin^2 \left(\frac{\delta m_{eff}^2 L}{4E} \right), \quad (8)$$

$$P(\nu_\mu \rightarrow \nu_e) = P(\nu_\mu \rightarrow \nu_\tau) = \frac{1}{2} \sin^2 2\theta \sin^2 \left(\frac{\delta m_{eff}^2 L}{4E} \right), \quad (9)$$

where $\sin \theta = |a_{ee} + a_{e\tau}| / \sqrt{2|a_{\mu\tau}|^2 + |a_{ee} + a_{e\tau}|^2}$. Therefore a maximal oscillation amplitude for ν_μ is possible but ν_μ oscillates equally to ν_e and ν_τ , which is excluded by atmospheric neutrino experiments. Hence this case is not allowed.

For Class 3F, the effective Hamiltonian is

$$h_{eff} = \begin{pmatrix} a_{ee} & c_{e\mu}E + a_{e\mu} & c_{e\tau}E + a_{e\tau} \\ c_{e\mu}E + a_{e\mu}^* & a_{\mu\mu} & c_{\mu\tau}E + a_{\mu\tau} \\ c_{e\tau}^*E + a_{e\tau}^* & c_{\mu\tau}E + a_{\mu\tau}^* & 0 \end{pmatrix}, \quad (10)$$

where $c_{e\mu}$ and $c_{\mu\tau}$ may be taken as real and positive, $c_{e\tau}$ is complex and $a_{\tau\tau}$ has been set equal to zero. In this case, for oscillations in atmospheric and long-baseline neutrinos, all three flavors have oscillation probability

$$P(\nu_\alpha \rightarrow \nu_\alpha) = \frac{5}{9} - 4|U_{\alpha 2}|^2 \left(\frac{2}{3} - |U_{\alpha 2}|^2 \right) \sin^2 \left(\frac{\delta m_{eff}^2 L}{4E} \right), \quad (11)$$

where U is the matrix that diagonalizes h_{eff} . This implies that all flavors of downward atmospheric neutrinos would be suppressed by a factor of 5/9, which is contrary to the data. Therefore this case is excluded.

Only three classes have the proper $1/E$ behavior *and* oscillation amplitudes for high energy neutrinos: 3B, 4D and 5B. For these cases we must check the predictions for solar and reactor neutrinos. As an example, for Class 3B we have

$$h_{eff} = \begin{pmatrix} c_{ee}E + a_{ee} & a_{e\mu} & c_{e\tau}E + a_{e\tau} \\ a_{e\mu}^* & 0 & a_{\mu\tau} \\ c_{e\tau}E + a_{e\tau}^* & a_{\mu\tau}^* & c_{\tau\tau}E + a_{\tau\tau} \end{pmatrix}, \quad (12)$$

where c_{ee} , $c_{\tau\tau}$ and $c_{e\tau}$ may be taken as real and $a_{\mu\mu}$ has been set to zero by a subtraction proportional to the identity. Degeneracy at order E requires $c_{\tau\tau} = r c_{e\tau} = r^2 c_{ee}$, where r is a free parameter. Then the oscillation probabilities for high-energy neutrinos are

$$P(\nu_\mu \rightarrow \nu_\mu) = 1 - \sin^2 2\theta \sin^2 \left(\frac{\delta m_{eff}^2 L}{4E} \right), \quad (13)$$

$$P(\nu_\mu \rightarrow \nu_e) = \sin^2 \phi \sin^2 2\theta \sin^2 \left(\frac{\delta m_{eff}^2 L}{4E} \right), \quad (14)$$

where $\tan \phi = r$ and $\tan \theta = \sqrt{1+r^2}|a_{e\mu}|/|ra_{ee} - a_{e\tau}|$. Maximal ν_μ oscillations are possible for $\theta \simeq \pi/4$, which imposes the condition $\sqrt{1+r^2}|a_{e\mu}| \simeq |ra_{ee} - a_{e\tau}|$.

Oscillations of ν_e at high energies must be small due to the limit on $\nu_\mu \rightarrow \nu_e$ from K2K [18] and MINOS [19]. For K2K and MINOS the oscillation amplitude for $P(\nu_\mu \rightarrow \nu_e)$, $\sin^2 \phi \sin^2 2\theta$, has an upper bound of about 0.14, which implies $r < 0.43$ for $\theta \simeq \pi/4$. The T2K experiment sees evidence for $\nu_\mu \rightarrow \nu_e$ at the 2.5σ level [20]; the T2K allowed regions are consistent with this bound.

For solar or reactor neutrinos the large energy limit does not apply. Adjusting the remaining free parameters, KamLAND data can be fitted reasonably well, as shown in Fig. 1. However, the fit is not as good as the standard oscillation scenario with neutrino mass.

Next we use these parameter values to check the solar phenomenology. Since the operator for a breaks CPT , we reverse the sign of a when we apply these parameter values to the solar neutrinos. However, the prediction does not agree with the solar data at high energies given the upper bound on r from above (see Fig. 2).

We also searched the a_{ee} , $a_{e\tau}$ and r parameter space to fit the solar data separately. The best fit still can not yield reasonable agreement with the solar data at high energies for $r < 0.43$ (see Fig. 3). If we do not impose the constraint on r , the fit to the solar data is improved at high energies. However, we cannot simultaneously fit the KamLAND and solar data even with larger r . We found that we also need $|a_{ee}|$ to become larger in order to fit the solar data, but larger $|a_{ee}|$ yields fast oscillations for KamLAND data with averaged probabilities around 1/2.

Classes 4D and 5B can also fit the KamLAND data, but not also solar data. Therefore no case can fit all of the data simultaneously.

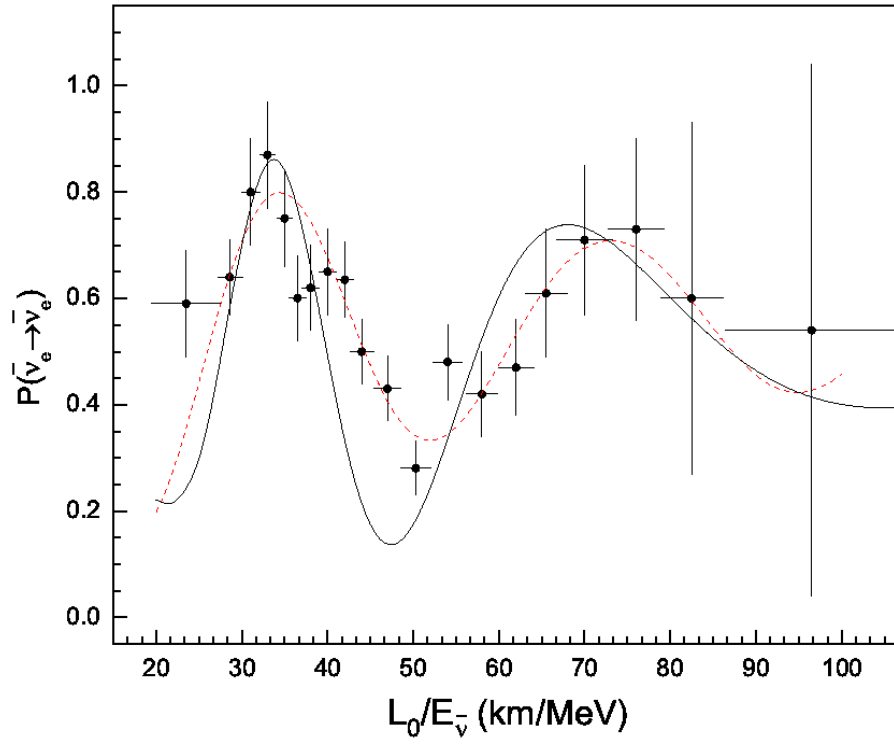


Figure 1: The best fit to the KamLAND data for Class 3B (solid lines) and the standard oscillation scenario with neutrino masses (dashed lines).

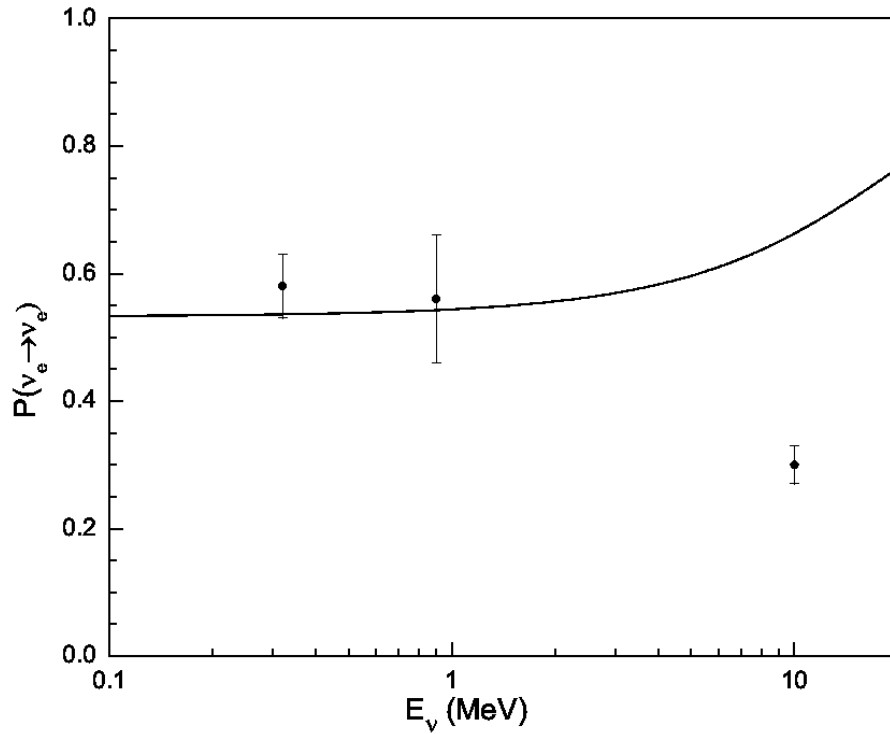


Figure 2: The prediction of Class 3B for the oscillation probability of solar neutrinos using the parameter values obtained from fitting KamLAND data [21]. The solar data points are from an update of the analysis in Ref. [22].

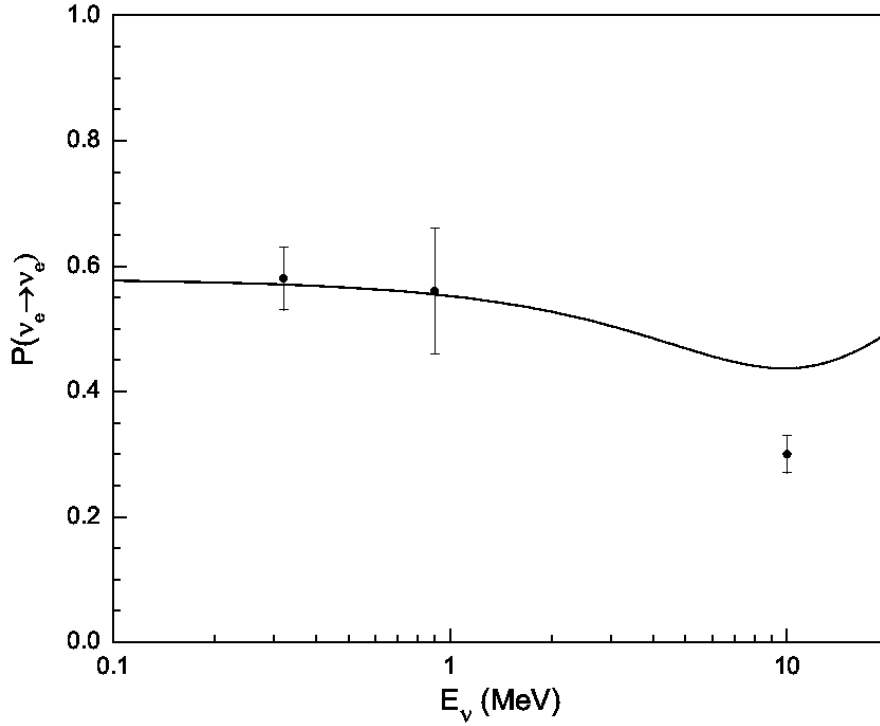


Figure 3: Best fit prediction for survival probability of ν_e for solar neutrinos for Class 3B, assuming $r < 0.43$.

4. Summary

We have examined the general three neutrino effective Hamiltonian in Eq. (1) for the case of direction-independent interactions and no neutrino mass. We looked for texture classes in which two eigenvalues were degenerate to order $1/E$ at high neutrino energy, so that oscillations of atmospheric and long-baseline neutrinos would exhibit the usual L/E dependence.

Among the classes that had the proper $1/E$ dependence at high energy, none was also able to fit the atmospheric, long-baseline, solar and KamLAND data simultaneously. Class 1A (along with the equivalent Classes 2A and 3A) reduced to the direction-independent bicycle model, which has been shown to be inconsistent with the solar, atmospheric and long-baseline neutrino data. Classes 2C (and the equivalent 3E) and 3F did not have the proper oscillation amplitudes for atmospheric neutrinos. Finally, Classes 3B (and the equivalent Classes 3C, 4A and 4D) and 5B (and the equivalent Class 6) were able to fit atmospheric and long-baseline neutrino data, but could not simultaneously fit KamLAND and solar data at lower neutrino energies. The major difficulty in these latter classes was reproducing the low survival probability of high-energy solar neutrinos.

Although we have not made an exhaustive search of the parameter space, the fact that high-energy neutrinos exhibit an L/E dependence in their oscillations over many orders of magnitude in E suggests that the only way this can occur in the effective Hamiltonian described by Eq. (1) is via the degeneracy of two eigenvalues to order $1/E$. Since none of the cases where such a degeneracy occurs are also able to fit all neutrino data simultaneously, it seems extremely unlikely that any direction-independent SME model without neutrino mass will provide a viable description of all neutrino oscillation phenomena. There is also strong evidence against direction-dependent terms. Furthermore, nonrenormalizable Lorentz noninvariant effective Hamiltonians with higher powers of energy (as in, *e.g.*, the model of Ref. [9]) and no neutrino masses would require additional degeneracy conditions. Therefore it appears highly unlikely that Lorentz invariance violation alone can account for all of the observed oscillation phenomena.

Acknowledgments

We thank Wan-yu Ye for computational assistance in the early stages of this work and A. Kostelecky for useful discussions. We also thank the Aspen Center for Physics for its hospitality during the initial stages

of this work. This research was supported by the U.S. Department of Energy under Grant Nos. DE-FG02-95ER40896, DE-FG02-01ER41155, and DE-FG02-04ER41308, by the NSF under Grant No. PHY-0544278, and by the Wisconsin Alumni Research Foundation.

References

- 1 See, *e.g.*, V. Barger, D. Marfatia and K. Whisnant, *Int. J. Mod. Phys. E* **12**, 569 (2003) [arXiv:hep-ph/0308123]; S. Pakvasa and J. W. F. Valle, *Proc. Indian Natl. Sci. Acad.* **70A**, 189 (2004) [arXiv:hep-ph/0301061].
- 2 D. Colladay, V. A. Kostelecky, *Phys. Rev.* **D55**, 6760-6774 (1997) [hep-ph/9703464]; *Phys. Rev.* **D58**, 116002 (1998) [hep-ph/9809521].
- 3 S. R. Coleman and S. L. Glashow, *Phys. Rev. D* **59**, 116008 (1999) [arXiv:hep-ph/9812418].
- 4 V. D. Barger, S. Pakvasa, T. J. Weiler and K. Whisnant, *Phys. Rev. Lett.* **85**, 5055 (2000) [arXiv:hep-ph/0005197].
- 5 T. Katori, V. A. Kostelecky and R. Tayloe, *Phys. Rev. D* **74**, 105009 (2006) [arXiv:hep-ph/0606154].
- 6 V. A. Kostelecky and M. Mewes, *Phys. Rev. D* **70**, 031902 (2004) [arXiv:hep-ph/0308300].
- 7 V. A. Kostelecky and M. Mewes, *Phys. Rev. D* **69**, 016005 (2004) [arXiv:hep-ph/0309025].
- 8 V. Barger, D. Marfatia and K. Whisnant, *Phys. Lett. B* **653**, 267 (2007) [arXiv:0706.1085 [hep-ph]].
- 9 J. S. Diaz and A. Kostelecky, *Phys. Lett. B* **700**, 25 (2011) [arXiv:1012.5985 [hep-ph]].
- 10 C. Athanassopoulos *et al.* [LSND Collaboration], *Phys. Rev. C* **54**, 2685 (1996) [arXiv:nucl-ex/9605001]; *Phys. Rev. Lett.* **77**, 3082 (1996) [arXiv:nucl-ex/9605003]; *Phys. Rev. C* **58**, 2489 (1998) [arXiv:nucl-ex/9706006]; *Phys. Rev. Lett.* **81**, 1774 (1998) [arXiv:nucl-ex/9709006]; A. Aguilar *et al.* [LSND Collaboration], *Phys. Rev. D* **64**, 112007 (2001) [arXiv:hep-ex/0104049].
- 11 A. A. Aguilar-Arevalo *et al.* [MiniBooNE Collaboration], *Phys. Rev. Lett.* **102**, 101802 (2009) [arXiv:0812.2243 [hep-ex]]; *Phys. Rev. Lett.* **103**, 111801 (2009) [arXiv:0904.1958 [hep-ex]]; *Phys. Rev. Lett.* **105**, 181801 (2010) [arXiv:1007.1150 [hep-ex]].
- 12 V. Barger, J. Liao, D. Marfatia, K. Whisnant, *Phys. Rev.* **D84**, 056014 (2011) [arXiv:1106.6023 [hep-ph]].
- 13 L. B. Auerbach *et al.* [LSND Collaboration], *Phys. Rev. D* **72**, 076004 (2005) [arXiv:hep-ex/0506067]; P. Adamson *et al.* [MINOS Collaboration], *Phys. Rev. Lett.* **101**, 151601 (2008) [arXiv:0806.4945 [hep-ex]]; *Phys. Rev. Lett.* **105**, 151601 (2010) [arXiv:1007.2791 [hep-ex]]; T. Katori [MiniBooNE Collaboration], arXiv:1008.0906 [hep-ph].
- 14 L. Wolfenstein, *Phys. Rev. D* **17**, 2369 (1978); V. D. Barger, K. Whisnant, S. Pakvasa and R. J. Phillips, *Phys. Rev. D* **22**, 2718 (1980); P. Langacker, J. P. Leveille and J. Sheiman, *Phys. Rev. D* **27**, 1228 (1983).
- 15 S. N. Ahmed *et al.* [SNO Collaboration], *Phys. Rev. Lett.* **92**, 181301 (2004) [arXiv:nucl-ex/0309004]; B. Aharmim *et al.* [SNO Collaboration], *Phys. Rev. C* **72**, 055502 (2005) [arXiv:nucl-ex/0502021]; *Phys. Rev. C* **75**, 045502 (2007) [arXiv:nucl-ex/0610020]; *Phys. Rev. Lett.* **101**, 111301 (2008) [arXiv:0806.0989 [nucl-ex]]; *Phys. Rev. C* **81**, 055504 (2010) [arXiv:0910.2984 [nucl-ex]].
- 16 See, *e.g.*, the global fits to neutrino data in T. Schwetz, M. A. Tortola and J. W. F. Valle, *New J. Phys.* **10**, 113011 (2008) [arXiv:0808.2016 [hep-ph]] (version 3 of the preprint, dated Feb. 11, 2010, presented an updated global analysis); M. C. Gonzalez-Garcia, M. Maltoni, J. Salvado, *JHEP* **1004**, 056 (2010). [arXiv:1001.4524 [hep-ph]]; G. L. Fogli, E. Lisi, A. Marrone, A. Palazzo, A. M. Rotunno, arXiv:1106.6028 [hep-ph].
- 17 Y. Ashie *et al.* [Super-Kamiokande Collaboration], *Phys. Rev. Lett.* **93**, 101801 (2004) [arXiv:hep-ex/0404034].
- 18 S. Yamamoto *et al.* [K2K Collaboration], *Phys. Rev. Lett.* **96**, 181801 (2006) [arXiv:hep-ex/0603004].
- 19 P. Adamson *et al.* [The MINOS Collaboration], *Phys. Rev.* **D82**, 051102 (2010) [arXiv:1006.0996 [hep-ex]]; *Phys. Rev. Lett.* **103**, 261802 (2009) [arXiv:0909.4996 [hep-ex]].
- 20 K. Abe *et al.* [T2K Collaboration], *Phys. Rev. Lett.* **107**, 041801 (2011) [arXiv:1106.2822 [hep-ex]].
- 21 T. Araki *et al.* [KamLAND Collaboration], *Phys. Rev. Lett.* **94**, 081801 (2005) [arXiv:hep-ex/0406035].
- 22 V. Barger, D. Marfatia and K. Whisnant, *Phys. Lett. B* **617**, 78 (2005) [arXiv:hep-ph/0501247].
- 23 S. Avvakumov *et al.*, *Phys. Rev. Lett.* **89**, 011804 (2002) [arXiv:hep-ex/0203018].